Inorganic Chemistry

COMMUNICATION

pubs.acs.org/IC

Proton-Induced Dynamic Equilibrium between Cyclometalated Ruthenium rNHC (Remote N-Heterocyclic Carbene) Tautomers with an NAD^+/NADH Function

Sumanta Kumar Padhi, Katsuaki Kobayashi, Shinya Masuno, and Koji Tanaka*

Department of Life and Coordination-Complex Molecular Science, Institute for Molecular Science, 5-1 Higashiyama, Myodaiji, Okazaki, Aichi 444-8787, Japan

Supporting Information

ABSTRACT: Cyclometalated ruthenium(II) complexes having acridine moieties have been synthesized and characterized by spectroscopic methods. Protonation of the acridine nitrogen of the ruthenium(II) complexes not only causes dynamic equilibrium with remote N-heterocyclic carbene Ru=C complexes but also generates the NAD^+/NADH redox function driven by a proton-coupled two-electron transfer accompanying a reversible C−H bond formation in the pyridinium ring.

A plethora of reports are available on complexes having N-heterocyclic carbene (NHC) ligands with Arduengo-type "classical" carbenes. On the contrary "nonclassical" NHCs are far less common.[1] Remote NHCs (rNHCs), derived from the pyridine-based ligands, are rarely known.[1a−d] We report the first acridine-based rNHC ruthenium complex with no heteroatoms in the carbene-containing ring and the nitrogen atom located in an adjacent aromatic ring. The σ-donating and π-accepting abilities of pyridine-based rNHCs are usually stronger than those of general imidazol-2-ylidines.[2] Pyridine-,[1a−k] quinoline-,[1d,l,m] and pyrazoline-based[1g] NHCs are being paid superior attention in the realms of carbene chemistry because of their inimitable structures and properties. The electron-rich carbon-centered neutral-donor rNHC-related palladium complexes are active catalysts in C−C coupling reactions.[3] Bergman, Carmona, Esteruelas, and Li groups have reported that some pyridines also undergo metal-induced rearrangements to form NHC ligands that involve tautomerization processes.[4]

Transition-metal complexes containing NAD^+/NADH hydride donors are rare.[5] One topic of organic chemistry that has flourished very recently involves reduction processes that use catalytic amounts of organic hydrides.[6] The development of catalytic reduction routes using organic hydrides derived from H_2O is currently a challenging aspect of this research.[6a] Electrolytic reduction processes have advantages in terms of cost and regulation of the reactivity of the catalysts by choosing applied potentials. Herein we report the synthesis, properties, dynamic equilibrium upon protonation, and catalytic activities of a cyclometalated ruthenium(II) complex with an NAD^+/NADH redox function as a hydride donor of H_2O origin.

The ligands 2-(pyridin-2-yl)acridine (**pad**) and 2-(pyridin-2-yl)-9,10-dihydroacridine (**padHH**) were synthesized using the synthetic procedures outlined in Scheme 1. The condensation of 2-pyridylcyclohexanone (**I**) with 2-aminobenzaldehyde (**II**) in the presence of KOH generates compound **III**, which upon dehydrogenation followed by hydrogenation with palladium/carbon in a *p*-cymene medium affords a mixture of **pad** and **padHH**. The treatment of either **pad** or **padHH** with $[(\eta^6\text{-}C_6H_6)RuCl_2]_2$, $NaPF_6$, and NaOH in acetonitrile provides $[Ru(\mathbf{pad})(CH_3CN)_4]PF_6$. In this case, the oxidation of **padHH** to **pad** took place even though the reaction was conducted in a nitrogen atmosphere. The further treatment of 2 equiv of 2,2′-bypiridyl (bpy) with $[Ru(\mathbf{pad})(CH_3CN)_4]PF_6$ in a 2-methoxyethanol medium gave $[Ru(\mathbf{pad})(\mathbf{bpy})_2]PF_6$ ($[\mathbf{1}]PF_6$).

Suitable single crystals of $[\mathbf{1}]PF_6$ for X-ray analysis could not be obtained, but it was isolated as the protonated form $[\mathbf{1H}](Cl)_2\cdot 10H_2O$ by the metathesis reaction with Bu_4NCl and was confirmed by X-ray crystallography. A perspective view of the molecular structure of $[\mathbf{1H}]^{2+}$ is displayed in Figure 1.

The complex $[\mathbf{1}]PF_6$ was reduced to $[\mathbf{1HH}]PF_6$ by both chemical as well as electrochemical methods. The purple color of $[\mathbf{1}]PF_6$ gradually turned to brownish-red under the controlled potential electrolysis at −1.5 V (vs SCE) in CH_3CN/H_2O [9:1 (v/v)] containing Bu_4NPF_6 as a supporting electrolyte (0.1 M), and $[\mathbf{1HH}]PF_6$ was produced after the consumption of 2 equiv of electrons in the electrolysis (Scheme 2). The cyclic voltammogram as well as the UV−vis spectrum of the resultant product are consistent with those of $[\mathbf{1HH}]PF_6$ obtained by the treatment of $[\mathbf{1}]PF_6$ with $NaBH_4$ in a methanol/H_2O mixture [9:1 (v/v)] under a nitrogen atmosphere. Yields of $[\mathbf{1HH}]PF_6$ by chemical reduction were better than those by the electrochemical method. The ^1H NMR spectrum of $[\mathbf{1HH}]PF_6$ in CD_3CN (Figure S5 in the Supporting Information) displayed 17 different signals with a total intensity of 29 protons, out of which 26 are in the aromatic region arising from two bpy and the **padHH** ligand. The NH proton peak appeared at 5.73 ppm and an AB-patterned doublet was observed at 3.95 ppm because of the germinal coupling of the methylene protons.

The **padHH** ligand is expected to coordinate in two different configurations with respect to the position of the carbon atoms in the acridine ring. The anti-coordination mode in $[Ru(\mathbf{pad})(CH_3CN)_4]PF_6$ and $[\mathbf{1}]PF_6$ was confirmed, as inferred from the three singlets of **pad** in the aromatic region of the ^1H NMR spectrum. Further it was also confirmed from X-ray crystallography. Sterically bulkier N-alkylated **padHH** ligands (***R***)-**padH**

Received: February 16, 2011
Published: May 26, 2011

Scheme 1. Synthesis of the Ligands

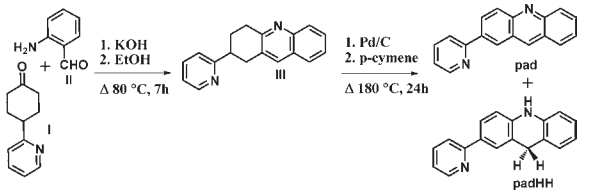

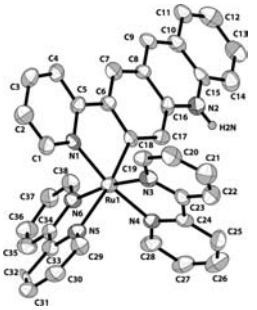

Figure 1. ORTEP (50% probability) of $[\mathbf{1H}]^{2+}$. Ru1−C18 [2.011(4) Å] and ^{13}C NMR of C18 appears at 228.87 ppm.

Scheme 2. Synthesis of $[\mathbf{1HH}]PF_6$

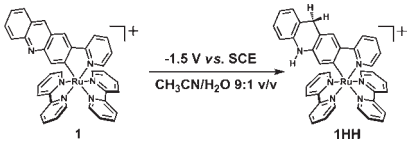

[10-(4-*tert*-butylbenzyl)-9,10-dihydro-2-(pyridin-2-yl)acridine and 10-(4-butylbenzyl)-9,10-dihydro-2-(pyridin-2-yl)acridine] were treated with $[(\eta^6\text{-}C_6H_6)RuCl_2]_2$ in a procedure similar to that of **padHH** to control the syn-coordination. Finally, it ends with the anti-coordination complex $[Ru(\mathbf{pad})(CH_3CN)_4]PF_6$ with oxidation of (***R***)-**padH** to **pad**. The anti-coordination makes a spare advantage in $[\mathbf{1HH}]PF_6$ to expose the methylene group, facilitating the reducing ability.

Each of these complexes exhibits the metal-to-ligand charge-transfer (MLCT) band in the visible region 400−600 nm along with the intraligand charge transfer in the UV region. The peaks appearing at 250−280 nm are of n → π^* (from **pad** and **padHH**) origin, and the $\pi \rightarrow \pi^*$ transitions occur in the 285−375 nm region. Under protic conditions, the UV−vis spectra of $[\mathbf{1}]PF_6$ show a bathochromic shift in the MLCT absorption band from 530 to 640 nm based on the **pad** ligand as the color changes from purple to green. It causes a decrease in the energy of the π^* orbital in **pad** after protonation, resulting in a red shift for the $Ru(t_{2g}) \rightarrow$ **pad**(π^*) orbital. The pK_a of $[\mathbf{1H}]^{2+}$ was determined to be 7.9 in water from the pH-dependent UV−vis spectra.

The X-ray crystallographic structure of $[Ru(\mathbf{padH})(CH_3CN)_4](PF_6)_2$ (Figure S28 in the Supporting Information) shows that the Ru−C bond distance is 1.965(9) Å, which is a consistent with a carbene-type coordination. The ^{13}C NMR peak of the coordinated carbon in nonprotonated complex $[Ru(\mathbf{pad})(CH_3CN)_4]PF_6$ appears at 129.43 ppm. It shifts downfield at 189.39 ppm upon protonation by the addition of 1 equiv of HCl. Similar behavior was also observed in $[\mathbf{1}]^+$, where the ^{13}C NMR peak appears at

Scheme 3. Dynamic Equilibrium between Ru−C and Ru═C

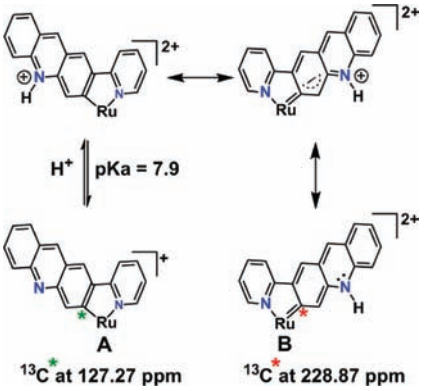

127.27 ppm and shifts to 228.87 ppm upon protonation. In $[\mathbf{1H}]Cl_2 \cdot 10H_2O$, the Ru−C bond [2.011(4) Å] is a significant feature of carbene-type behavior. Upon protonation, the Ru−C bond exists in tautomeric equilibrium with Ru═C coordination (Scheme 3). The electronic structure of the protonated complex may be an intermediate canonical form of the contributing structures Ru^{II}−C and Ru^{IV}═C. In this case, the π-accepting ability of the coordinated carbon center increases upon protonation because of a decrease in the energy of the π^* orbital in **pad** after protonation compared to the nonprotonated form. Although ^{13}C NMR signals of the allenylidene-type Ru═C═C bond appear at 287−315 ppm,[7] those of rNHC are reported in the range of 170−200 ppm.[1] In $[\mathbf{1HH}]PF_6$, the ^{13}C NMR peak appears at 126.57 ppm, which is consistent with Ru−C-type single-bond character.

The dynamic equilibrium between the Ru−C bond and Ru═C coordination was also supported by the temperature-dependent ^{1}H NMR of $[\mathbf{1}]PF_6$ with the addition of 1 equiv of HCl. The signal of the adjacent proton to the coordinated carbon center undergoes a shielding effect with a lowering of the temperature, signifying an increase in the Ru═C-type contribution.

$$\underset{\text{A}}{\text{Ru—C}} \overset{K}{\rightleftharpoons} \underset{\text{B}}{\text{Ru=C}} \qquad (1)$$

The equilibrium constant of eq 1 is defined as $K = (1 - x)/x$, where $x = [\delta_{obs} - \delta(B)]/[\delta(A) - \delta(B)]$ [δ(A) and δ(B) are the chemical shifts of the A and B species]. Computer simulation using $\delta(A) = 7.33$ and $\delta(B) = 7.12$ for the adjacent proton to the coordinated carbon center at higher and lower temperature, respectively, gave the most reasonable linear plot of ln K vs T^{-1} (Figure 2). The standard enthalpy change $\Delta H°$ and the standard entropy change $\Delta S°$ were determined to be −4.93 cal mol^{-1} and −21.82 cal K^{-1} mol^{-1}, respectively, from the Vukancic−Vukovic equation.

The cyclic voltammogram of $[\mathbf{1}]PF_6$ in dry CH_3CN exhibits two reversible Ru^{II}/Ru^{III} and Ru^{III}/Ru^{IV} redox couples at $E_{1/2}$ = +0.52 and +0.78 V (vs SCE), respectively (Figure S22 in the Supporting Information). A broad cathodic wave appears at −1.61 V as a shoulder of one of the two reversible (bpy, bpy/bpy$^{\bullet-}$, bpy) and (bpy$^{\bullet-}$, bpy/bpy$^{\bullet-}$, bpy$^{\bullet-}$) redox couples at $E_{1/2}$ = −1.64 and −1.92 V, respectively. The addition of 1 equiv of water to the solution shifted the cathodic peak at −1.61 to −1.50 V, which further underwent an anodic shift with increasing amounts of water, and one cathodic wave emerged at −1.10 V in CH_3CN/H_2O

dx.doi.org/10.1021/ic200315f |*Inorg. Chem.* 2011, 50, 5321–5323

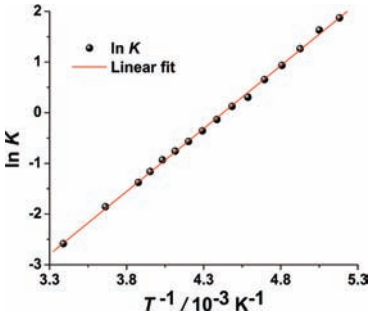

Figure 2. Plot of ln K vs T^{-1} for the dynamic equilibrium between Ru−C and Ru═C upon protonation.

(9:1, v/v). Consumption of two Faraday per 1 mol of electrons in the exhaustive electrolysis of the resultant solution at −1.20 V clarified the irreversible redox reaction as a proton-coupled two-electron reduction of **pad**, affording **padHH**. In the case of [**1HH**]PF_6, the two redox couples at −1.61 and −1.85 V were respectively due to the reduction of (bpy, bpy/bpy$^{\bullet-}$, bpy) and (bpy$^{\bullet-}$, bpy/bpy$^{-\bullet}$, bpy$^{-\bullet}$) (Figure S24 in the Supporting Information). An irreversible oxidation wave was observed at the anodic end at +0.45 V with the couple at −0.61 V, assigned to **padHH**-based oxidation along with the reversible redox couple for Ru^{II}/Ru^{III} at +0.90 V.

The complex [**1**]PF_6 also acts as an organic hydride donor for the reduction of benzaldehyde as well as acetophenone under electrochemical conditions at −1.20 and −1.40 V (vs SCE), respectively, in CH_3CN/H_2O (7:3, v/v), which is similar to the enzymatic NAD^+/NADH redox reaction driven by proton-coupled two-electron reduction accompanying a reversible C−H bond formation in the pyridinium ring. Acetophenone and benzaldehyde are reduced electrochemically at more negative potentials (−1.5 V). Therefore, the controlled potential of [**1**]PF_6 in CH_3CN/H_2O (7:3, v/v) was conducted at −1.4 and −1.2 V, respectively, for the substrates, although the reaction rate was slow. Under these conditions, the yield is very mild, and the turnover numbers for the reduction of acetophenone and benzaldehyde are around 1 and 4, respectively.

The Ru−C bond upon protonation exists in tautomeric equilibrium with Ru═C coordination. The role of [**1**]PF_6 is similar to the enzymatic NAD^+/NADH reaction driven by a proton-coupled two-electron reduction accompanying a reversible C−H bond formation in the pyridinium ring. This system has led to the first successful path to generate and release hydride ions from an NADH-analogous **padHH** in a ruthenium(II) complex. It behaves as an organic hydride donor toward the reduction of benzaldehyde and acetophenone with two electrons and H_2O as the proton source. In this case, the σ-donating and π-accepting ability of an electron-rich carbon-centered ligand **pad** is usually stronger than that of its corresponding N-coordinating analogues. It is subject to enhancement in the reducing activities with a susceptibility of change in the oxidation state at the metal center through a proton-coupled resonance. Thus, an important feature is to find a metal complex system that acts as the biomimic of the NAD^+/NADH-type "hydride" donor.

■ ASSOCIATED CONTENT

Ⓢ Supporting Information. Experimental details and crystallographic data in CIF format. This material is available free of charge via the Internet at http://pubs.acs.org.

■ AUTHOR INFORMATION

Corresponding Author
*E-mail: ktanaka@ims.ac.jp.

■ ACKNOWLEDGMENT

This work is supported by a Grand-in-Aid for Specially Promoted Research (Grant 20002005) from the Ministry of Education, Culture, Sports, Science, and Technology of Japan.

■ REFERENCES

(1) (a) Stander-Grobler, E.; Schuster, O.; Heydenrych, G.; Cronje, S.; Tosh, E.; Albrecht, M.; Frenking, G.; Raubenheimer, H. G. *Organometallics* **2010**, *29*, 5821–5833. (b) Schuster, O.; Yang, L.; Raubenheimer, H. G.; Albrecht, B. *Chem. Rev.* **2009**, *109*, 3445–3478. (c) Raubenheimer, H. G.; Cronje, S. *Dalton Trans.* **2008**, 1265–1272. (d) Schuster, O.; Raubenheimer, H. G. *Inorg. Chem.* **2006**, *45*, 7997–7999. (e) Han, Y.; Huynh, H. V.; Tan, G. K. *Organometallics* **2007**, *26*, 6581–6585. (f) Iglesias-Sigüenza, J.; Ros, A.; Díez, E.; Alcarazo, M.; Álvarez, E.; Fernández, R.; Lassaletta, J. M. *Dalton Trans.* **2009**, 7113–7120. (g) Cabeza, J. A.; Del Río, I.; Goite, M. C.; Pérez-Carreño, E.; Pruneda, V. *Chem.—Eur. J.* **2009**, *15*, 7339–7349. (h) Song, G.; Zhang, Y.; Su, Y.; Deng, W.; Han, K.; Li, X. *Organometallics* **2008**, *27*, 6193–6201. (i) Cabeza, J. A.; del Río, I.; Pérez-Carreño, E.; Sánchez-Vega, M. G.; Vázquez-García, D. *Angew. Chem., Int. Ed.* **2009**, *48*, 555–558. (j) Cabeza, J. A.; del Río, I.; Pérez-Carreño, E.; Sánchez-Vega, M. G.; Vázquez-García, D. *Organometallics* **2010**, *29*, 4464–4471. (k) Cabeza, J. A.; del Río, I.; Pérez-Carreño, E.; Pruneda, V. *Chem.—Eur. J.* **2010**, *16*, 5425–5436. (l) Meyer, W. H.; Deetlefs, M.; Pohlmann, M.; Scholz, R.; Esterhuysen, M. W.; Julius, G. R.; Raubenheimer, H. G. *Dalton Trans.* **2004**, 413–420. (m) Esteruelas, M. A.; Fernández-Alvarez, F. J.; Oñate, E. *Organometallics* **2007**, *26*, 5239–5245.

(2) (a) Gómez-Bujedo, S.; Alcarazo, M.; Pichon, C.; Alvarez, E.; Fernández, R.; Lassaletta, J. M. *Chem. Commun.* **2007**, 1180–1182. (b) Hahn, F. E.; Jahnke, M. C. *Angew. Chem., Int. Ed.* **2008**, *47*, 3122–3172.

(3) Schneider, S. K.; Roembke, P.; Julius, G. R.; Loschen, C.; Raubenheimer, H. G.; Frenking, G.; Herrmann, W. A. *Eur. J. Inorg. Chem.* **2005**, 2973–2977.

(4) (a) Conejero, S.; Lara, P.; Paneque, M.; Petronilho, A.; Poveda, O.; Serrano, M. L.; Batiré, F.; Alvarez, E.; Moya, C.; Salazar, V.; Carmona, E. *Angew. Chem., Int. Ed.* **2008**, *47*, 4380–4383. (b) Alvarez, E.; Conejero, S.; Paneque, M.; Petronilho, A.; Poveda, O.; Serrano, M. L.; Carmona, E. *J. Am. Chem. Soc.* **2006**, *128*, 13060–13061. (c) Buil, M. L.; Esteruelas, M. A.; Garcés, K.; Oliván, M.; Oñate, E. *J. Am. Chem. Soc.* **2007**, *129*, 10998–10999.

(5) (a) Matsubara, Y.; Koga, K.; Kobayashi, A.; Konno, H.; Sakamoto, K.; Morimoto, T.; Ishitani, O. *J. Am. Chem. Soc.* **2010**, *132*, 10547–10552. (b) Fukushima, T.; Fujita, E.; Muckerman, J. T.; Polyansky, D. E.; Wada, T.; Tanaka, K. *Inorg. Chem.* **2009**, *48*, 11510–11512. (c) Polyansky, D. E.; Cabelli, D.; Muckerman, J. T.; Fukushima, T.; Tanaka, K.; Fujita, E. *Inorg. Chem.* **2008**, *47*, 3958–3968. (d) Kimura, M.; Tanaka, K. *Angew. Chem., Int. Ed.* **2008**, *47*, 9768–9771. (e) Tannai, H.; Koizumi, T.; Wada, T.; Tanaka, K. *Angew. Chem., Int. Ed.* **2007**, *46*, 7112–7115. (f) Polyansky, D.; Cabelli, D.; Muckerman, J. T.; Fujita, E.; Koizumi, T.; Fukushima, T.; Wada, T.; Tanaka, K. *Angew. Chem., Int. Ed.* **2007**, *46*, 4169–4172. (g) Koizumi, T.; Tanaka, K. *Angew. Chem., Int. Ed.* **2005**, *44*, 5891–5894. (h) Kobayashi, A.; Konno, H.; Sakamoto, K.; Sekine, A.; Ohashi, Y.; Iida, M.; Ishitani, O. *Chem.—Eur. J.* **2005**, *11*, 4219–4226. (i) Kobayashi, A.; Takatori, R.; Kikuchi, I.; Konno, H.; Sakamoto, K.; Ishitani, O. *Organometallics* **2001**, *20*, 3361–3363.

(6) (a) Xu, H.-J.; Liu, Y.-C.; Fu, Y.; Wu, Y.-D. *Org. Lett.* **2006**, *8*, 3449–3451. (b) Imada, Y.; Iida, H.; Naota, T. *J. Am. Chem. Soc.* **2005**, *127*, 14544–14545.

(7) Wong, C.-Y.; Lai, L.-M.; Lam, C.-Y.; Zhu, N. *Organometallics* **2008**, *27*, 5806–5814 and references cited therein.